

## Systematic Investigations on the Effect of Divalent Metal Ions (Mg<sup>2+</sup> and Zn<sup>2+</sup>) Substitution on Nanocrystalline Manganese Ferrites

G. Vasuki<sup>1,\*</sup>, T. Balu<sup>2</sup>

<sup>1</sup> *Research scholar, Reg. no: 9282, S.T. Hindu College, Nagercoil-629002, affiliated to Manonmaniam Sundaranar University, Tirunelveli-627012, Tamilnadu, India*  
<sup>2</sup> *Associate Professor and Head, Department of Physics, Aditanar College of Arts and science, Tiruchendur, affiliated to Manonmaniam Sundaranar University, Tirunelveli-627012, Tamilnadu, India*

(Received 18 October 2018; revised manuscript received 06 February 2019; published online 25 February 2019)

Mg<sup>2+</sup> and Zn<sup>2+</sup> substituted manganese ferrite nanoparticles were synthesized by chemical co-precipitation route. The synthesized samples were characterized by powder X-ray diffraction which confirms the cubic spinel ferrite structure and the crystallite size is in nanoscale. High resolution transmission electron microscope and scanning electron microscope were used to examine the surface morphology. The elemental composition and purity of the sample were confirmed from energy dispersive X-ray spectroscopic analysis. The band gap energy determined from UV-Vis absorption spectra reveals the semiconducting behavior of both the samples. The optical parameters calculated from the UV-Vis absorption spectra show that MMF has better optical property compared to ZMF nanocrystallites. The magnetic parameters determined using vibrating sample magnetometer show low coercivity, low squareness ratio exhibiting superparamagnetic behavior of the Mg<sup>2+</sup> and Zn<sup>2+</sup> substituted manganese ferrite nanoparticles which are important for technological applications.

**Keywords:** Co-precipitation, Diffraction, Morphology, Coercivity, Superparamagnetism.

DOI: [10.21272/jnep.11\(1\).01021](https://doi.org/10.21272/jnep.11(1).01021)

PACS numbers: 61.46.Df, 68.37.Og, 75.60.Ej

### 1. INTRODUCTION

Tremendous research work has been going on to synthesize applications oriented pure and mixed nanoferrites. These ferrites are an important group of metal oxide magnetic materials used in variety of applications, such as inductor cores, sensors, magnetic information storage, microwave devices, magnetic resonance imaging, cancer treatment, pollution control, catalysis, etc. [1, 2]. Progressive researches are carried out to prepare highly pure, good quality, technologically important ferrite nanoparticles. Spinel ferrites are excellent magnetic materials due to their versatile nature, high stability and reduced cost, greater electronic and magnetic performance over an extended range of frequencies [3]. The properties of nanoferrites are largely different from their bulk counterparts due to their quantum confinement and larger surface area.

For further improvement, ferrites can be doped with other divalent and trivalent metal ions. Mg<sub>0.5</sub>Zn<sub>0.5-x</sub>Cu<sub>x</sub>Fe<sub>2</sub>O<sub>4</sub>, Mn<sub>1-x</sub>Zn<sub>x</sub>Fe<sub>2</sub>O<sub>4</sub>, Mg<sub>1-x</sub>Co<sub>x</sub>Fe<sub>2</sub>O<sub>4</sub> are some of the commonly synthesized ferrites by various synthesis techniques, such as co-precipitation, combustion, hydrothermal, solgel, microemulsion and so on [4-7]. Any synthesis method depends on various factors, such as concentration of dopant, pH, temperature, stirring velocity, etc., which have to be maintained as the preparation forms an important basis in determining the properties of the nanomaterials [8]. Chemical co-precipitation is one of the simplest, low temperature techniques yielding good quality nanopowders in large amount. In this method, an appropriate ratio of metal ions was taken, which are precipitated at desired pH and temperature. Mixed manganese ferrites are partially inverse spinel in structure as a result of which they are used practically compared to other ferrites. In order to achieve specific improved properties they are doped with other magnetic and nonmagnetic ions.

Magnesium and zinc are some appropriate divalent metal ions that can be doped with manganese ferrites, as it is expected to improve the behavior and shall be put to use for device fabrication [9, 10].

In the present work, Mg<sup>2+</sup> and Zn<sup>2+</sup> substituted manganese nanoferrites (MMF and ZMF respectively) were synthesized by chemical co-precipitation technique. The as-synthesized samples have been characterized for their structural, morphological, optical and magnetic properties. The results are compared and discussed in detail.

### 2. MATERIALS AND METHODS

#### 2.1 Synthesis

Mixed MMF and ZMF were synthesized by chemical co-precipitation technique using highly pure analytical reagents of sulphate salts of M<sup>2+</sup> (Mg<sup>2+</sup>, Zn<sup>2+</sup>), Mn<sup>2+</sup> and Fe<sup>3+</sup> with sodium hydroxide (NaOH) as precipitant and deionized water as solvent. Aqueous solutions of M<sup>2+</sup>, Mn<sup>2+</sup> and Fe<sup>3+</sup> were taken in the stoichiometric ratio 0.5:0.5:2. This is stirred continuously for 30 minutes to form the starting solution with pH ~ 3. The starting solution is precipitated by dropwise addition of NaOH until the pH reaches 11. The formed precipitate is stirred continuously for 2 hours maintaining a temperature of 70 °C to get a uniform phase of spinel ferrites. The obtained precipitate is washed repeatedly, filtered and dried at 150 °C. This is further grinded to get MMF and ZMF nanopowders.

#### 2.2 Characterization

The as-synthesized MMF and ZMF nanopowders were characterized to study the structure, morphology, optical and magnetic behavior. Structural analysis was made from powder X-ray diffraction (pXRD) studies

obtained using XPERT – PRO diffractometer system with CuK $\alpha$  radiation of wavelength 1.5406 Å. The crystallite size, shape and morphology were analyzed using high resolution transmission electron microscope (HRTEM) (Model: JEOL/JEM 2100). Further, surface morphology was observed from the micrographs obtained from scanning electron microscope (SEM) (Model: JEOL/JSM 6390). To verify the elements present and to determine their composition, energy dispersive X-ray (EDAX) spectra was taken along with SEM. UV-Vis absorption spectrum in the wavelength range of 190 nm to 1100 nm was recorded using UV-Vis spectrophotometer, from which the band gap energy was determined. Using Lakeshore 7410 model vibrating sample magnetometer (VSM) the magnetic analysis at room temperature was made in the field range of – 15000 to + 15000G.

### 3. RESULTS AND DISCUSSION

#### 3.1 Structural and Morphological Analysis

The X-ray diffraction is an effective analysis to determine the structure of a material. The pXRD patterns of as-synthesized MMF and ZMF samples are shown in Fig. 1. They exhibit strong widened peaks due to the reflections at the planes that agree with JCPDS 89-4924 of MgFe<sub>2</sub>O<sub>4</sub> and JCPDS 89-1012 of ZnFe<sub>2</sub>O<sub>4</sub> nanoparticles. No impurity peaks were observed. This confirms the cubic ferrite nanocrystalline structure of MMF and ZMF nanoparticles.

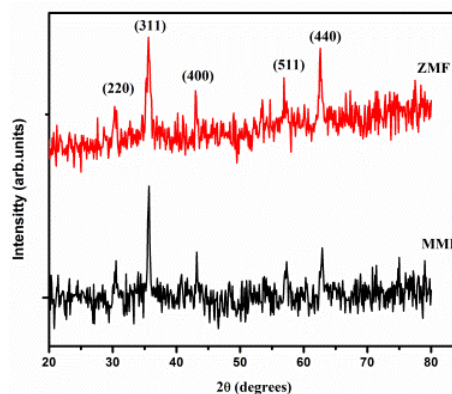


Fig. 1 – Powder XRD pattern of MMF and ZMF nanoparticles

The various lattice parameters from XRD data were calculated using the relations discussed elsewhere [11]. The values are given in Table 1 and Table 2.

The lattice constant ( $a$ ) of MMF is lesser than ZMF due to the fact that the ionic radius of Mg<sup>2+</sup> (0.66 Å) is smaller than Zn<sup>2+</sup> (0.74 Å). The X-ray density ( $\rho_x$ ) of MMF is smaller than ZMF due to very low density of Mg<sup>2+</sup> (1.741 g/cm<sup>3</sup>) compared to Zn<sup>2+</sup> (7.140 g/cm<sup>3</sup>). The distance between the magnetic ions or the hopping lengths corresponding to the tetrahedral site ( $L_A$ ) is greater than the value of the octahedral site ( $L_B$ ) for both the samples as they depend purely on the lattice constant. Also the hopping lengths of MMF are lesser than the hopping lengths of ZMF nanocrystallites.

Table 1 – Values of lattice parameters determined from XRD analysis

| Sample | $2\theta$ (311 plane) | $a$ , Å | $V$ , Å <sup>3</sup> | $\rho_x$ , g/cm <sup>3</sup> | $L_A$ , Å | $L_B$ , Å |
|--------|-----------------------|---------|----------------------|------------------------------|-----------|-----------|
| MMF    | 35.5578               | 8.3738  | 587.18               | 4.8708                       | 3.6260    | 2.9606    |
| ZMF    | 35.3884               | 8.4126  | 595.36               | 5.2618                       | 3.6428    | 2.9743    |

Table 2 – Values of crystallite size, surface area, dislocation density and microstrain

| Sample | Crystallite size, nm |       | $d$ -spacing, Å            |                | $S \cdot 10^3$ , m <sup>2</sup> /g | $\rho_D \cdot 10^{14}$ , m <sup>-2</sup> | $\epsilon_s \cdot 10^{-3}$ |
|--------|----------------------|-------|----------------------------|----------------|------------------------------------|--|----------------------------|
|        | $D$                  | $D_T$ | XRD                        | SAED           |                                    |  |                            |
| MMF    | 18                   | 4.5   | 1.704 (422)<br>2.521 (311) | 1.742<br>2.57  | 72.46                              | 34.6                                     | 6.87                       |
| ZMF    | 19                   | 4.9   | 3.027 (220)<br>1.465 (440) | 2.865<br>1.473 | 60.02                              | 27.7                                     | 5.50                       |

The crystallite size ( $D$ ) calculated using the Scherrer's relation shows that both MMF and ZMF are in nano-scale. The specific surface area ( $S$ ) of both the samples is large, which leads to better mechanical properties. The dislocation density ( $\rho_D$ ), a measure of dislocations in a unit volume of a crystalline material is large due to the smaller size of the MMF and ZMF nanoparticles. The microstrain ( $\epsilon_s$ ) that is produced due to the defects and stress in the synthesized materials is high due to the large surface showing the nanosize of the particles. The values of surface area, dislocation density and microstrain of MMF nanoparticles are larger than those of ZMF nanoparticles as the values depend on the crystallite size. HRTEM is a direct observation of particle's appearance. Fig. 2 (a)-(b) shows HRTEM micrographs of MMF and ZMF, respectively. The morphology exhibits spherical profile of the two samples with some agglomerations due to the weak surface interaction, such

as Van der Waals forces between the particles [12]. The average crystallite size ( $D_T$ ) of both the samples is about 5 nm (Table 2). The diffraction rings observed from SAED pattern (see Fig. 2 (c)-(d)) explain the crystalline nature of the materials. The  $d$ -spacing values determined from the diffraction rings are in good agreement with the  $d$ -spacing values determined through XRD and given in Table 2. The materials clearly exhibit the cubic spinel structure as explained in XRD.

SEM micrographs of MMF and ZMF nanocrystallites are shown in Fig. 3(a)-(b), respectively. The images reveal spherical morphology of both the samples. As seen in HRTEM, the particles are observed to be agglomerated in the SEM images. EDAX in the energy range from 0 to 20 keV (see Fig. 4(a)-(b)) show the chemical composition of elements present in Mg<sup>2+</sup> and Zn<sup>2+</sup> substituted manganese nanoferrites. The elements manganese (Mn), magnesium (Mg), zinc (Zn), iron (Fe) and

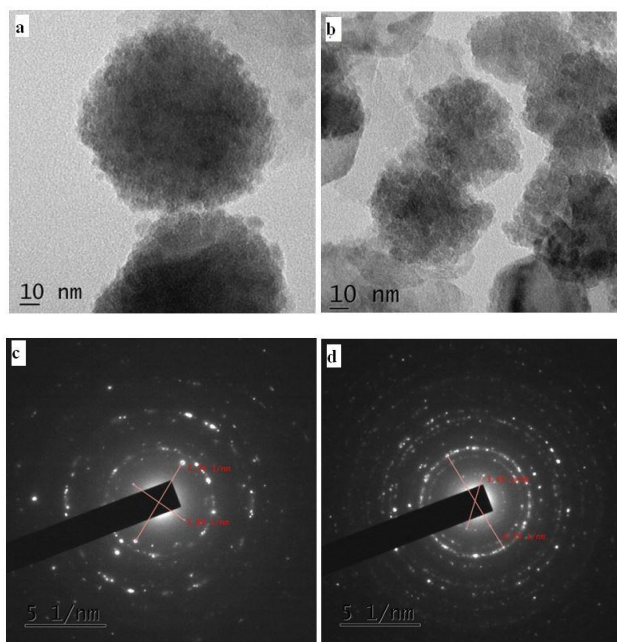


Fig. 2 – TEM MMF image (a), ZMF image (b), SAED MMF pattern (c) and SAED MMF pattern (d)

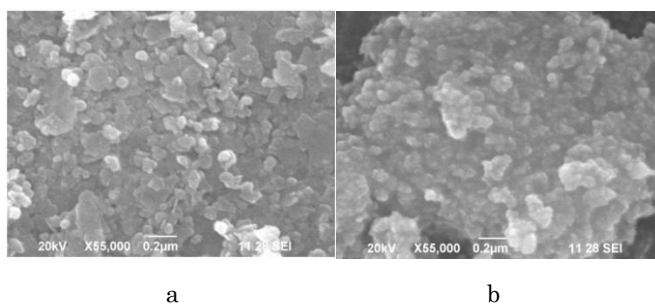


Fig. 3 – SEM images of MMF(a) and ZMF (b)

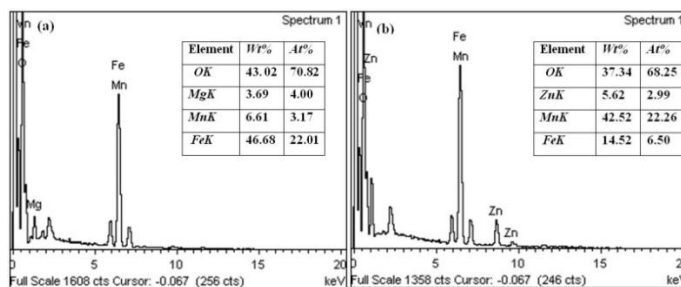


Fig. 4 – EDAX pattern of MMF (a) and ZMF (b)

oxygen (O) present in each sample were observed with no impurity components confirming the desired formation of MMF and ZMF nanoparticles. The weight percentage of the elements is given as insets in Fig. 4(a)-(b).

### 3.2 Optical studies

In order to analyze the optical behavior of the synthesized materials, UV-Vis absorption studies have been carried out. UV-Vis absorption spectrum has been recorded in the wavelength range of 190-1100 nm for MMF and ZMF as shown in Fig. 5. The absorptions observed at 392.55 nm for MMF and 383.85 nm for ZMF inform that the size of the particles are in nanoscale for both the samples, since absorptions in this

range originate mainly from the absorption of UV radiation by magnetic nanoparticles [13].

Band gap energy  $E_g$  (Table 3) was directly calculated using the Planck's relation:

$$E_g = hc/\lambda, \tag{1}$$

where  $h$  is the Planck's constant,  $c$  is the velocity of light and  $\lambda$  is the cutoff wavelength. The band gap energy of MMF is less than of ZMF due to the reduced crystallite size of MMF compared to ZMF. Also the values explain the semiconducting nature of the synthesized materials. To understand the optoelectronic behavior of a material, refractive index ( $n$ ) acts as an essential parameter. Using band gap energy, the value of

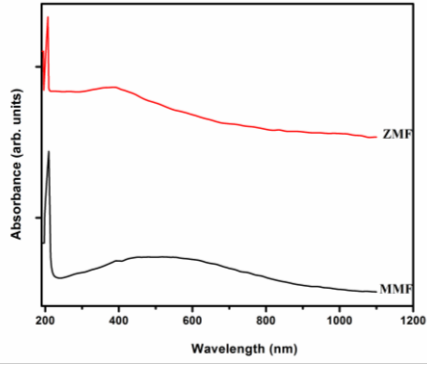


**Fig. 5** – UV-Vis spectra of MMF and ZMF nanoparticles

$n$  can be determined using the relation given by Moss as suggested by Gupta and Ravindra [14]

**Table 3** – Optical parameters determined from UV-Vis analysis

| Sample | $\lambda$ , nm | $E_g$ , eV<br>$hc/\lambda$ | $n$         |              | $\epsilon_\infty$ |                 |
|--------|----------------|----------------------------|-------------|--------------|-------------------|-----------------|
|        |                |                            | Moss method | Anani method | By Moss method    | By Anani method |
| MMF    | 209.4          | 5.93                       | 2.07        | 2.21         | 4.27              | 4.90            |
| ZMF    | 206.9          | 6.00                       | 2.06        | 2.20         | 4.24              | 4.84            |

**Table 4** – Magnetic parameters determined from hysteresis curve

| Sample | $M_s$ , emu/g | $H_c$ , G | $M_r$ , emu/g | $M_r/M_s$ | $M_B(\mu_B)$ |
|--------|---------------|-----------|---------------|-----------|--------------|
| MMF    | 25.7214       | 78.278    | 2.6258        | 0.1021    | 0.9917       |
| ZMF    | 32.3146       | 6.058     | 0.1687        | 0.0052    | 1.3646       |

### 3.3 Magnetic Studies

Magnetic property of nanoferrites depends on the particle's surface, cation distribution, spin order, synthesis method etc. [17]. In order to analyze the magnetic behavior of the synthesized materials, magnetic studies at room temperature were carried out using VSM. The obtained hysteresis curves of MMF and ZMF nanoparticles are shown in Fig. 6. The curves exhibit the soft magnetic nature of both MMF and ZMF nanoparticles.

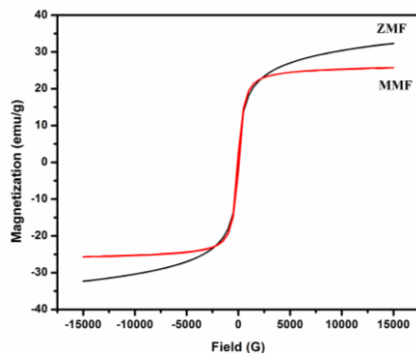


**Fig. 6** – Comparison of hysteresis curves of MMF and ZMF nanoparticles

Saturation magnetization  $M_s$ , coercivity  $H_c$  and retentivity  $M_r$  were obtained from the hysteresis curve and are given in Table 4. The saturation magnetization varies due to the exchange interaction of the cations in tetrahedral (A) and octahedral (B) sites. Neel's theory insists that the effective magnetization is the difference in magnetization of the two sites with the B sublattice having a higher magnetization [18]. The saturation

$$E_g n^4 = k, \quad (2)$$

where  $k = 108$  eV is a constant. Also Anani et al. have suggested an empirical relation for refractive index of semiconducting solids [15]. The relation is:

$$n = \frac{17 - E_g}{5}. \quad (3)$$

The relations are found to give values in better agreement with known data of semiconducting materials [16]. It is observed that the refractive index increases with decrease in the band gap energy as expected. The optical dielectric constant, which is the square of refractive index ( $\epsilon_\infty$ ), increases as the band gap energy decreases. This is an opt result showing enhanced optical properties.

magnetization values are smaller than bulk ferrites ( $\sim 80$  emu/g) for both ZMF and MMF nanoparticles. The ZMF nanoparticles show very low value of coercivity, which indicates the excellent superparamagnetic behavior which is an important requirement for technological applications. The high value of coercivity of MMF might be due to the spin disorder that may occur on the surface and within the cores of the nanoparticles due to vacant sub-lattice disorder sites of  $Fe^{3+}$  at the tetrahedral site [19].

The small value of squareness ratio ( $M_r/M_s$ ) (Table 4) indicates the presence of non-interacting single domain particles with cubic anisotropy in nanoferrites. The magnetic moment ( $M_B$ ) is calculated from the molecular weight ( $M_w$ ) and the saturation magnetization – using the relation:

$$M_B = \frac{M_w \cdot M_s}{5585}. \quad (4)$$

The variation of the magnetic moment (see Table 4) is in correlation with magnetization as expected. The magnetic moment in ferrites might vary from the theoretical values, because the distribution of cations might vary when the crystallite is reduced to nanosize.

The magnetic analysis shows that the magnetic quantities are distinguishable for manganese ferrites when substituted by  $Mg^{2+}$  and  $Zn^{2+}$  divalent ions.

## 4. CONCLUSIONS

The mixed spinel structured MMF and ZMF nanoparticles were chemically synthesized successfully by coprecipitation technique. The pXRD studies confirm cubic spinel ferrite nanostructures and high purity of the syn-

thesized samples. The HRTEM micrographs results are compared with XRD results, and they are in good agreement. The diffraction rings observed in SAED patterns further confirm the crystalline structure of MMF and ZMF nanoparticles. Spherical morphology of the synthesized samples was further confirmed from SEM images. The EDAX pattern of all the samples shows the presence of corresponding elements and their composition with no impurities exhibiting the purity of the obtained nanoferrites. The optical parameters calculated from the UV-Vis absorption spectra show that MMF has better optical property compared to ZMF nanocrystallites. The magnetic

analysis of both the samples exhibits superparamagnetic behavior, and the low value of squareness ratio contributes to electromagnetic applications.

#### ACKNOWLEDGMENTS

The authors would like to thank XRD facility, Manonmaniam Sundaranar University, Tirunelveli for XRD studies, STIC, Cochin for HRTEM analysis, Karunya University for SEM and EDAX analysis and UV-Vis studies and SAIF, IIT Madras for VSM studies.

#### REFERENCES

1. R.P. Araujo-Neto, E.L. Silva-Freitas, J.F. Carvalho, T.R.F. Pontes, K.L. Silva, I.H.M. Damasceno, E.S.T. Egito, Ana L. Dantas, Marco A. Morales, Artur S. Carrico, *J. Magn. Magn. Mater.* **364**, 72 (2014).
2. Richa Srivastava, B.C. Yadav, *Int. J. Green Tech.* **4**, 141 (2012).
3. I.A. Vedernikova, *Review J. Chem.* **5** 256 (2015).
4. H.M. Zaki, S.Al. Heniti, Ahmad Umar, F. Al-arzouki, A. Abdel-Daiem, T.A. Elmosalami, H.A. Dawoud, F.S. Al-Hazmi, S.S. Ata-Allah, *J. Nanosci. Nanotech.* **13**, 4056 (2013).
5. Yimin Xuan, Qiang Li, Gang Yang, *J. Magn. Magn. Mater.* **312**, 464 (2007).
6. M. Anis-ur Rehman, Muhammad Ali Malik, M. Akram, M. Kamran, Kishwar Khan, Asghari Maqsood, *J. Supercond. Nov. Magn.* **25**, 2691 (2012).
7. Muhammad Khurram Abbas, Muhammad Azhar Khan, Faiza Mushtaq, Muhammad Farooq Warsi, Muhammad Sher, Imran Shakir, Mohamed F. Aly Aboud, *Ceram. Int.* **43**, 5524 (2017).
8. Zhuang Yuan, Zhen-hua Chen, Ding Chen, Zhi-tao Kang, *Ultrasonics Sonochem.* **22**, 188 (2015).
9. R. Arulmurugan, G. Vaidyanathan, S. Sendhilkathan, B.Jeyadevan, *J. Magn. Magn. Mater.* **298**, 83 (2006).
10. H. Mohseni, H. Shokrollahi, Ibrahim Sharifi, Kh. Gheisari, *J. Magn. Magn. Mater.* **324**, 3741 (2012).
11. G. Vasuki, T. Balu, *Mater. Res. Express* **5**, 065001 (2018).
12. Manju Kurian, Smitha Thankachan, Divya S. Nair, E.K. Aswathy, Aswathy Babu, Arathy Thomas, K.T. Binu Krishna, *J. Adv. Ceramics* **4**, 199 (2015).
13. Obaid ur Rahman, Subash Chandra Mohapatra, Sharif Ahmad, *Mater. Chem. Phys.* **132**, 196 (2012).
14. N.M. Ravindra, Preethi Ganapathy, Jinsoo Choi, *Infrared Phys. Technol.* **100**, 715 (1980).
15. M. Anani, C. Mathieu, S. Lebid, Y. Amar, Z. Chama, H. Abid, *Comp. Mater. Sci.* **41**, 570 (2008).
16. N. Bouarissa, *Physica B* **399**, 126 (2007).
17. S. Ayyappan, S. Mahadevan, P. Chandramohan, M.P. Srinivasan, John Philip, Baldev Raj, *J. Phys. Chem. C* **114**, 6334 (2010).
18. L. Neel, *Ann. Phys.* **3**, 137 (1948).
19. V. Manikandan, A. Vanitha, E. Ranjith Kumar, J. Chandrasekaran, *J. Magn. Magn. Mater.* **432**, 477 (2017).

### Систематичні дослідження впливу заміщення іонів дивалентних металів ( $Mg^{2+}$ та $Zn^{2+}$ ) на нанокристалічні марганцеві ферити

G. Vasuki<sup>1</sup>, T. Balu<sup>2</sup>

<sup>1</sup> Research scholar, Reg. no: 9282, S.T. Hindu College, Nagercoil-629002, affiliated to Manonmaniam Sundaranar University, Tirunelveli-627012, Tamilnadu, India

<sup>2</sup> Associate Professor and Head, Department of Physics, Aditanar College of Arts and science, Tiruchendur, affiliated to Manonmaniam Sundaranar University, Tirunelveli-627012, Tamilnadu, India

Заміщені  $Mg^{2+}$  і  $Zn^{2+}$  у наночастинках фериту марганцю були синтезовані шляхом хімічного співосадження. Синтезовані зразки характеризувалися порошковою рентгенівською дифракцією, що підтверджує кубічну структуру фериту шпінелі, а розмір кристалітів знаходиться у нанодіапазоні. Для дослідження морфології поверхні використовувалися просвічуючий електронний мікроскоп з високою роздільною здатністю та скануючий електронний мікроскоп. Елементний склад і чистоту зразка підтверджували за допомогою енергодисперсійного рентгенівського спектроскопічного аналізу. Ширина забороненої зони, визначена зі спектрів поглинання УФ та видимого діапазонів, виявляє напівпровідникову поведінку обох зразків. Магнітні параметри, визначені за допомогою вібраційного магнітометра, демонструють низьку коерцитивність та низький коефіцієнт прямокутності, що показує суперпарамагнітну поведінку заміщених  $Mg^{2+}$  і  $Zn^{2+}$  наночастинок, є важливими для технологічних застосувань. Встановлено наявність відповідних елементів та їх склад без домішок, які демонструють чистоту отриманих наноферритів. Оптичні параметри, розраховані зі спектрів поглинання УФ та видимого діапазонів, показують, що нанокристаліт MMF має кращу оптичну властивість порівняно з нанокристалітами ZMF.

**Ключові слова:** Співосадження, Дифракція, Морфологія, Коерцитивність, Суперпарамагнетизм